Original
ISSN 2413-0516

Anti-Inflammatory Humulene-Type Sesquiterpenoids from *Asteriscus Graveolens*

Hajer S. Alorfi[1], Fayza A. Aljohany[1], Fatima B. Alamri[2], Hanan I. Althagbi[3], Ashraf B. Abdel-Naim[4], Walied M. Alarif[5*], Fitri Budiyanto[6], Esam M. Aboubakr[7]

[1]Department of Chemistry, Faculty of Science, King Abdulaziz University, PO. Box 80203, Jeddah 21589, Saudi Arabia.
[2]Department of Chemistry, faculty of Science, Bisha University, Abha, PO Box 62562, Saudi Arabia.
[3]Department of Chemistry, College of Science, University of Jeddah, Jeddah 21589, Saudi Arabia.
[4]Department of Pharmacology and Toxicology, Faculty of Pharmacy, King Abdulaziz University, Jeddah 21589, Saudi Arabia.
[5]Department of Marine Chemistry, Faculty of Marine Sciences, King Abdulaziz University, PO. Box 80207, Jeddah 21589, Saudi Arabia.
[6]Research Center for Vaccine and Drugs, National Research and Innovation Agency (BRIN), Bogor, 16911, Indonesia.
[7]Department of Pharmacology and Toxicology. Faculty of Pharmacy, South Valley University, Qena83523, Egypt.
*Correspondence to: Walied M. Alarif (E-mail: welaref@kau.edu.sa)
(Submitted: 26 August 2024 – Revised version received: 11 September 2024 – Accepted: 04 October 2024 – Published online: 26 October 2024)

Abstract

Objective: Inflammation is the initial physiological reaction of the immune system to infection or irritation, leading significant risk factors for several forms of cancer. The genus *Asteriscus* has been observed to possess a notable abundance of sesquiterpenes with anti-inflammatory properties. This study was designed to assess the anti-inflammatory activity of the sesquiterpenoids isolated from *Asteriscus graveolens*.

Methods: The organic extract of the Asteraceae plant A. graveolens was subjected to different chromatographic and spectroscopic techniques for isolation, purification, and identification of sesquiterpenoid contents. The isolated compounds were screened for anti-inflammatory activities in two animal models: rat paw edema and rat ear edema. Histopathological examinations as well as biochemical markers of inflammation were assessed. This was followed by in silico screening for anti-inflammatory activity.

Results: Four known sesquiterpenoids were isolated from *A. graveolens*, including two humulene derivatives, namely, 9-oxohumula-4-en-6,15-olide (**1**), and 9-oxohumula-1(10)(*Z*),4,7(*E*)-trien-6,15-olide (**2**) and two bisabolene derivatives, identified as bisabola-2,10-dien-1-one (**3**) and 6- hydroxybisabola-2,10-dien-1-one (**4**) described. In the rat paw edema model, compound **2** showed highest activity in preventing formation carrageenan-induced paw edema. This was confirmed by histopathological examinations that indicated partial preservation of the epidermal and dermal layers. Further, the compound significantly inhibited cyclooxygenase-2 (COX-2) and tumor necrosis factor-α (TNF-α) release. In the croton oil indued rat ear edema, compounds **2** and **4** significantly inhibited ear edema and protected against histopathological alterations. This was associated with prevention of myeloperoxidase (MPO) concentration in ear tissues. Molecular docking and molecular dynamic simulation indicated the affinity and docking stability of compounds **1**–**4** to the selected inflammatory protein.

Conclusion: Phytochemical investigation of *A. graveolens* resulted in the isolation and characterization of four sesquiterpenes. In particular, compound **2** showed potent anti-inflammatory activity in carrageenan rat paw edema and croton oil ear edema.

Keywords: Asteraceae, terpenoids, lactones, croton oil, spectroscopy

Introduction

Inflammation is the initial physiological reaction of the immune system to infection or irritation. The term 'inflammation' originates from the Latin word "inflammo," which translates to "I set alight, I ignite".[1] Moreover, inflammation can be triggered by various factors such as physical injury, exposure to ultraviolet radiation, invasion by microorganisms, and immunological responses. The primary characteristics of inflammation include erythema, thermogenesis, edema, and nociception. Inflammatory cascades can result in the occurrence of diseases such as persistent asthma, rheumatoid arthritis, multiple sclerosis, inflammatory bowel disease, and psoriasis.[2] Inflammation can be classified into two main types based on timing and clinical features: acute and chronic. Chronic inflammatory disease is defined by the presence of ongoing inflammation and chronic inflammation refers to a gradual alteration in the composition of cells at the location of the inflammatory response. It is characterized by both the destruction and repair of the damaged tissue occurring simultaneously.[1,3] In contrast, acute inflammation manifests during short time intervals ranging from seconds to days and it is marked by the heightened migration of plasma and cells from the innate immune system, such as neutrophils and macrophages, from the bloodstream to the damaged tissues.[3] Chronic inflammation is a known precursor to the development of cancer. Recent experimental and clinical research have provided evidence to support this idea, which is now widely accepted worldwide. Epidemiological studies have revealed persistent infections and inflammation as significant risk factors for several forms of cancer.[2]

The utilization of plants, their components, or extracts as anti-inflammatory agents has been recognized since ancient times. An example of a substance utilized in Arab folk medicine for many years is a concentrated, thick liquid extract made from ripe carob (*Ceratonia siliqua* L.). This extract is well known for its effectiveness in treating mouth inflammations.[4] Plants have served as the foundation for numerous traditional medical systems worldwide for millennia and persist in offering humanity novel cures.[2] Additionally, Essential oils of flora plants are being recognized as a valuable source of bioactive natural compounds that can effectively combat inflammation. Many studies on the anti-inflammatory effects

of substances are conducted in rodents using various experimental models such as carrageenan, formalin, and arachidonic acid-induced paw edoema. Additionally, in vitro and ex vivo procedures may be used, which can involve the use of essential oils.[3]

The genus Asteriscus is classified within the Inula group of the plant family Asteraceae-Inuleae. The genus under discussion, together with two other genera belonging to the same tribe (*Ighermia Wiklund* and *Pallenis Cass.*), collectively encompass a total of 15 species that exhibit natural growth patterns in coastal and desert regions across the Mediterranean and Middle East.[5,6] Moreover, two species, *Asteriscus aquaticus and Asteriscus graveolens*, have a wide distribution, particularly in the Mediterranean region. The remaining six species exhibit highly limited regional ranges.[7] Additionally, the plant genus is renowned for its compounds that include potential antispasmodic, anticancer, and anti-inflammatory properties, which are employed in the treatment of infected wounds. Moreover, the findings of the antimicrobial investigation on the extract revealed a wide range of antibacterial activity against gram-positive bacteria, gram-negative bacteria, and fungal cultures.[8] Based on existing literature, it has been observed that *Asteriscus* genera exhibit a notable abundance of flavonoids, phenolics, sesquiterpenes, bisabolone and hydroperoxides.[8] The vast majority of the sesquiterpenes that have been extracted from *Asteriscus* plants have a humulene moiety, indicating that this attribute serves as a chemotaxonomic property for the entire *Asteriscus* genus.[9]

Asteriscus graveolens (Forssk.) Less. is a plant species that is also known by the synonyms *Bubonium graveolens*, *Odontospermum graveolens* or *Nauplius graveolens*[5] and known under the names of "Nougd" in Arabic.[10] *Asteriscus graveolens*, a member of the Asteraceae family, is classified as a perennial sub-shrub. This species is an indigenous aromatic medicinal herb that grows in desert regions of Asia and North Africa.[5,11] It has been used as a stomachic, for treating fever, gastrointestinal tract symptoms, cephalic aches, bronchitis, Anti-diabetic, bowel diseases, diuretic, hypotensive, depurative and as an anti-inflammatory agent in Saharan traditional medicine.[12] The main sesquiterpene lactones found in *A. graveolens* are humulanolides, which consist of the asteriscanolide and aquatolide skeletons, characterised by a unique γ-lactone group. These compounds have promising pharmacological actions, possess fascinating chemical structures, and act as a precursor for the development of more intricate structures, which piques the attention of synthetic chemists.[13]

Despite the widespread use *of A. graveolens*, it is remarkable that there are no reports in the literature regarding its anti-inflammatory qualities. Thus, in the present study, we report for the first time the anti-inflammatory agent of the sesquiterpenes obtained from aerial parts of *A. graveolens*.

Results

Chemistry

Chromatographic investigation of *A. graveolens* led to the identification of four sesquiterpenes, identified as 9-oxohumula-4-en-6,15-olide (**1**), and 9-oxohumula-1(10)(*Z*),4,7(*E*)-trien-6,15-olide (**2**), bisabola-2,10-dien-1-one **(3)** and 6-hydroxybisabola-2,10-dien-1-one **(4)** (Figure 1).

9-Oxohumula-4-en-6,15-olide (**1**): crystalline material (mp 112–115°C); HRFAB-MS 273.9819 [M + Na]$^+$, 250.1580 (calcd. 250.1569) [M$^+$,$C_{15}H_{22}O_3$]; HREI-MS, 250.1580 [M$^+$,$C_{15}H_{22}O_3$]; ^{1}H-NMR ($CDCl_3$,850 MHz) and ^{13}C-NMR ($CDCl_3$, 850 MHz) (Tables 1 and 2); HRESIMS: (calculated for *m/z* = 250.1569 for $C_{15}H_{22}O_3$) [9, 14].

9-Oxohumula-1(10)(*Z*),4,7(*E*)-trien-6,15-olide (**2**) crystalline material (mp 156–157 °C); ^{1}H-NMR ($CDCl_3$,850 MHz) and ^{13}C-NMR ($CDCl_3$, 850 MHz) (Tables 1 and 2); HRESIMS: (calculated for *m/z* = 246 for $C_{15}H_{18}O_3$).[14–16]

Bisabola-2,10-dien-1-one (**3**): colourless oil; ^{1}H-NMR ($CDCl_3$, 850 MHz) and ^{13}C-NMR ($CDCl_3$,850 MHz) (Tables 1 and 2); HRESIMS: (calculated for *m/z* = 220 for $C_{15}H_{24}O$).[17]

6-Hydroxybisabola-2,10-dien-1-one (**4**): colourless oil; ^{1}H-NMR ($CDCl_3$, 850 MHz) and ^{13}C-NMR ($CDCl_3$,850 MHz) (Tables 1 and 2); HRESIMS: (Calculated for *m/z* = 236 for $C_{15}H_{24}O_2$).[17]

Biology

Impact of the isolated compounds on Carrageenan-induced rat paw edema

The data in Table 3 indicate that compound **2** and indomethacin significantly inhibited carrageenan-induced edema in rat

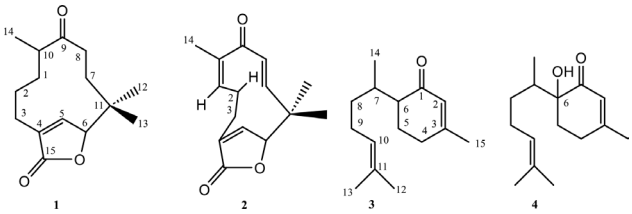

Fig. 1 **Sesquiterpenes from *A. graveolens*.**

Table 1. **1H NMR spectral data of compounds 1–4**

P	1	2	3	4
	δ_H m *J* (Hz)	δ_H m *J* (Hz)	δ_H m *J* (Hz)	δ_H m *J* (Hz)
1	1.63 m 1.88m	6.02 m	–	–
2	1.41m 1.81m	2.70 m 2.35 m	5.86 brs	5.86 brs
3	2.08 2.18 brt (13)	2.20 m	–	–
4	–	–	2.32 m 2.19 dt	2.35–2.25m
5	7.0 s	7 brs	1.92 m 1.80 m	1.8 m
6	4.5 s	4.70 brs	2.36 m	3.6 s
7	1.45 m 1.85m	6.15 d (14.1)	1.78 m	1.70 tq
8	2.46 m 2.57 m	5.29 d (14.1)	1.72 m 1.30 m	1.30 m
9	–	–	2.03 m 1.98 m	1.98 m
10	2.56 m	–	5.11 brt (7.2)	4.98 brt (6.5)
11	–	–	–	–
12	1.1 s	1.40 s	1.60 brs	1.64 brs
13	1.2 s	1.20 s	1.68 brs	1.56 brs
14	1.0 d (7)	1.90 brs	0.79 d (6.9)	1.02 d (6.5)
15	–	–	1.93 brs	1.95 brs

Table 3. **13C NMR spectral data of compounds 1–4**

P	1	2	3	4
1	32.0	138.3	201.2	203
2	23.5	29.9	124.5	124.3
3	25.2	23.0	161.3	162.6
4	134.3	138.8	30.9	32
5	147.5	147.9	30.2	30
6	45.0	88.0	49.8	77
7	28.4	136.5	34.7	34
8	35.0	133.0	26.0	26
9	213.5	198.5	25.7	25.6
10	44.8	133.7	127.2	123.2
11	41.0	42.6	131.5	131.4
12	23.8	30.0	24.2	25.9
13	29.3	24.7	15.6	17.6
14	18.5	21.3	17.7	13.1
15	173.5	138.3	22.3	24

paws. These inhibitions were 22.2 and 31.4% respectively as compared to the carrageenan alone treatment group.

Histopathological examinations of rat paws

Examination of rat paws in the control group revealed normal histological structure of dermis and epidermis (Figure 2A). However, carrageenan injection resulted in diffuse dermal necrosis with infiltration by inflammatory cells mainly neutrophils and lymphocytes (Figure 2B). Animals treated with compounds **1**, **3**, and **4** showed moderate dermal necrosis with infiltration by mononuclear inflammatory cells (Figure 2 C, E, and F respectively). It is noteworthy to report that pre-treatment with compound 2 or indomethacin exhibited mild focal dermal necrosis and mild dermal infiltration by mononuclear inflammatory cells (Figure 2D and F respectively).

Effect of the isolated compound on TNF-α release in rat paw exudate of carrageenan-induced rats

Intraplantar injection of carrageenan resulted in a 2.4 and 5.6-fold increase in the release of COX-2 and TNF-α respectively, in rat paw exudate. Compounds **1** and **3** did not affect carrageenan-induced rise in COX-2. Nevertheless, all the screened compounds showed significant inhibition of TNF-α release. Compound **2** showed inhibitory activities comparable to those observed in the indomethacin group as it significantly prevented COX-2 and TNF-α release by 55 and 60% respectively (Figure 3A and B).

Effect of the isolated compounds on croton oil-induced ear edema

As shown in Table 4, application of croton oil to rat ears significantly the development of inflammatory edema as it enhanced the ear punch weight by 127.7% as compared to control animals. All the screened compounds showed variable degrees of protection against croton oil-induced inflammation. Compound **2** and indomethacin showed the best protective activities as they prevented the rise in the ear punch weight by 27.6 and 38.7% respectively as compared to carrageenan alone treatment group.

Histopathological examination of Croton oil-induced ears

Histopathological examination of ear tissues obtained from control animals revealed the normal histological structure of the epidermis, dermis, and ear cartilage (Figure 4A). However, the application of croton oil resulted in severe hemorrhage with infiltration by mononuclear inflammatory cells in the dermal layer (Figure 4B). Ear sections from animals pre-treated with compounds **1**, **3**, and **4** indicated the presence of moderate hemorrhage with severe edema (Figure 4C, E, F). Both compound **2** and indomethacin treatment groups exhibited mild dermal edema with infiltration by a low number of mononuclear inflammatory cells (Figure 4D and G).

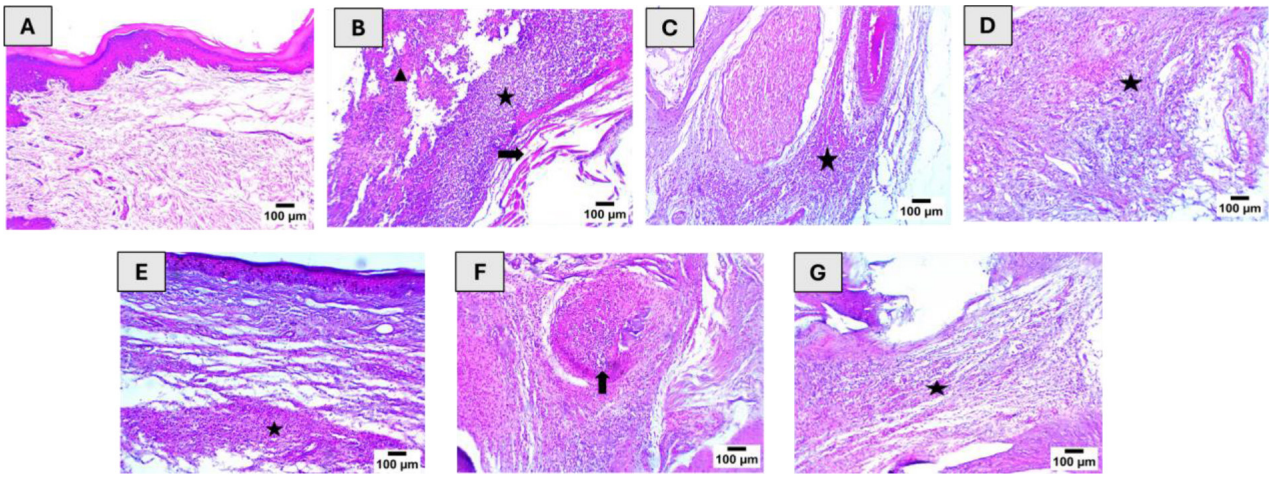

Fig. 2 **Effect of the isolated compounds on histopathological changes in Carrageenan-induced rat paw edema experiment. Plate A (Control) shows the normal architecture of the dermis and epidermis of the rat paw. Plate B (Carrageenan) shows diffuse dermal necrosis with infiltration by inflammatory cells mainly neutrophils and lymphocytes. Plates C–F; corresponding to com-pounds 1, 2, 3, and 4 respectively show moderate to mild dermal necrosis with infiltration by mononuclear inflammatory cells. Plate F (Indomethacin) illustrates mild dermal infiltration by mononuclear inflammatory cells. Arrowheads indicate severe dermal necrosis. Stars indicate in-flammatory cell infiltration. Arrows indicate the presence of edema in the muscular layer (He-matoxylin and Eosin stain).**

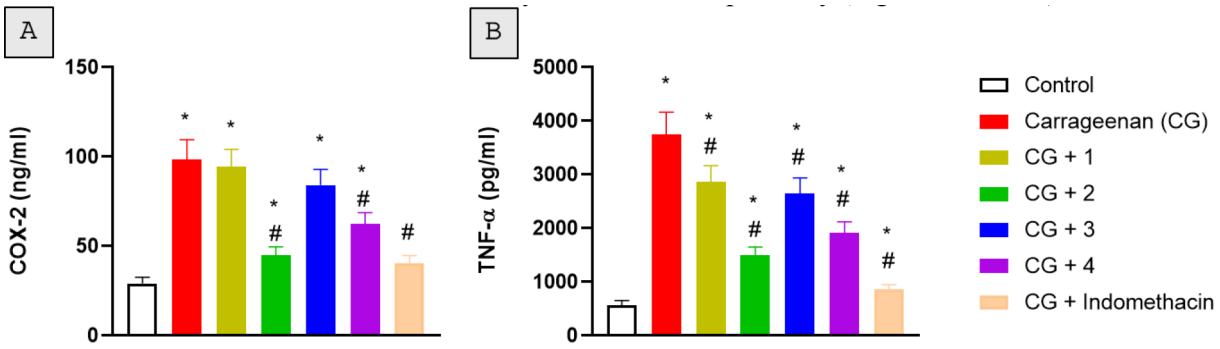

Fig. 3 **Effect of the isolated compounds on COX-2 (A) and TNF-α (B) release in rat paw exudate of carrageenan-challenged rats. * Statistically significant from the control group at $P < 0.05$. # Statistically significant from the Carrageenan-induced group at $P < 0.05$.**

Table 4. **Effect of the isolated compounds on Carrageenan-induced Rat paw edema**

Group	Paw volume (mL)	Edema inhibition (%)
Control	0.97 ± 0.04	–
Carrageenan (CG)	1.53* ± 0.07	–
CG + 1	1.51* ± 0.12	1.3
CG + 2	1.19 *, # ± 0.07	22.2
CG + 3	1.47* ± 0.11	3.9
CG + 4	1.40*± 0.10	8.5
Indomethacin (10 mg/Kg)	1.05# ± 0.09	31.4

* Significantly different from control at $P<.05$
\# Significantly different from CG at $P<.05$.

Effect of the isolated compounds on MPO activity in ear tissues of croton oil-induced rats

As shown in Figure 5, the application of croton oil significantly caused a 2.3fold increase in MPO activity in ear tissues. However, all the screened compounds showed significant protective activities against the increase in MPO activity. In this regard, compound **2** and indomethacin exhibited the most potent activities as they significantly inhibited MPO activity by 46.6 and 56.9% respectively, as compared to the croton oil alone group.

In silico study

Molecular docking

Compounds **1–4** demonstrated binding affinity to the selected proteins, as indicated by their negative binding affinity values in all experiments. Among them, compound **2** exhibited the strongest affinity for 2AZ5, 4OTJ, and 1CXP, with binding affinities < -7.30 kcal/mol. Notably, the binding affinity of compound **2** to 4OTJ was higher than that of indomethacin, a standard anti-inflammatory compound. Additionally, all compounds showed affinity for MAPK, 5-LOX, and particularly COX-1, suggesting potential alternative pathways for their mechanisms of action (Table 5).

The docking of compounds **1–4** was facilitated through hydrogen bonds and hydrophobic interactions with specific protein residues. Compound **2** docking to TNFα (2AZ5) was stabilised by one hydrogen bond and four hydrophobic interactions, whereas its docking to COX-2 and MPO involved two hydrogen bonds (Figure 6). Notably, compound **1** docking to TNFα was supported by just one hydrogen bond, with no additional interactions observed (Figure 7).

Molecular docking

Molecular dynamic simulation was carried out for compounds **1–4** to TNFα (2AZ5), COX-2 (4OTJ), and MPO (1CXP) within 100 ns observation. Compounds **1–4** exhibited stable docking within 100 ns with RMSD < 2 Å within the simulation duration (Figure 8A–C). All residue of the selected protein also indicated RMSF < 2 Å while docked to compounds **1–4** (Figure 8D–F). This molecular dynamic simulation implies that these compounds may inhibit the activity of the proteins.

Discussion

Sequential chromatographic techniques of extraction and purification of the organic extract of the Asteraceae member, *Asteriscus graveolens*, afforded four pure isolates based on thin layer chromatography examination. Positive response up on spraying with *p*-anisaldehyde reagent revealed the possibility of existence of four sesquiterpenoids.

Compound **1** was isolated as a crystalline material. ^{13}C-NMR spectrum referred to the presence of fifteen carbon signals. HRESIMS indicated the molecular formula $C_{15}H_{22}O_3$ (five unsaturation sites). ^{1}H-NMR spectrum showed the presence of a singlet olefinic proton resonating at δ_H 7.0, two tertiary methyl at 1.20 and 1.10, and a secondary methyl at 1.00 (J = 7 Hz) ppm. DEPT experiments indicated the presence of four quaternary carbons resonating at δ_C 213.5 (carbonyl carbon), 173.5, 134.3, and 41.0; three methine carbon signals at δ_C 147.5, 45, and 44.8, five methylene signals, and three methyl signals (Table 2). The presence of three double-bond characters assigned the bicyclic structure of compound **1**. The presence of an α-substituted lactone was deduced from the carbonyl-lactone at 173.5, the low-field methine at δ_C 147.5; δ_H 7.0. The in-hand spectral data unambiguously referred to the presence of a humulane-carbon skeleton and the current data are coincided with those reported by Rauter et al. 2016 for the compound 9-Oxohumula-4-en-6,15-olide (**1**).

Compound **2** was isolated as a crystalline material. ^{13}C-NMR spectrum referred to the presence of fifteen carbon signals. HRESIMS indicated the molecular formula $C_{15}H_{18}O_3$ (seven unsaturation sites). ^{1}H-NMR spectrum showed the presence of four olefinic protons resonating at δ_H 7.0, 6.15, 6.02, and 5.19, three tertiary methyl at 1.90, 1.40 and 1.20 ppm. The obtained spectral data clearly showed that

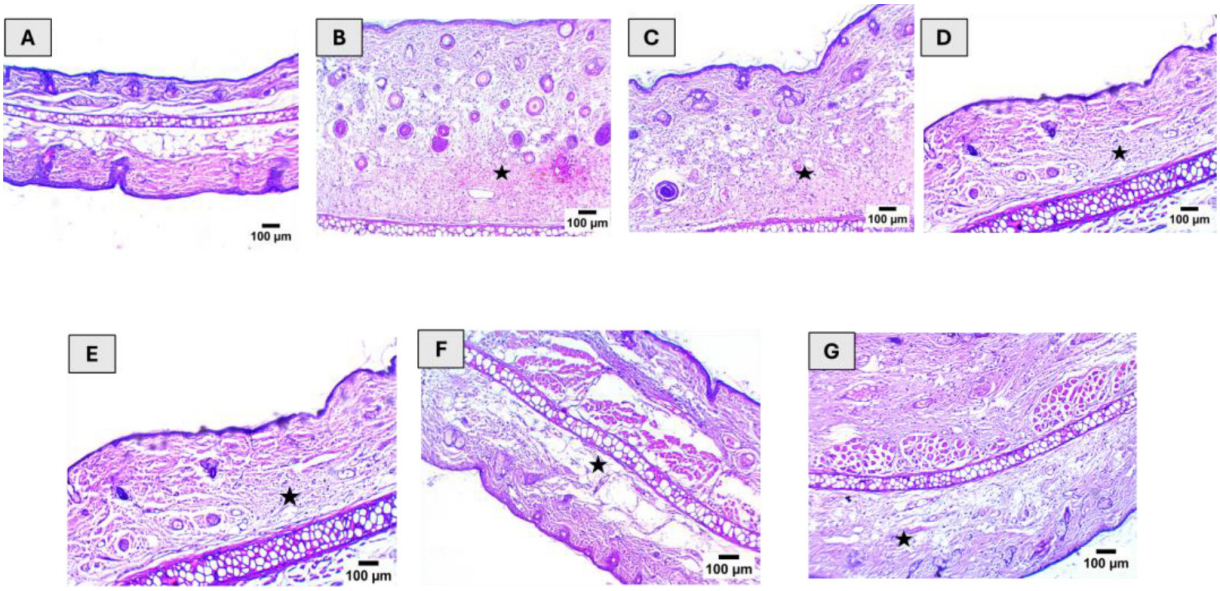

Fig. 4 **Effect of the isolated compounds on histopathological changes in Croton oil-induced ear edema. Sub-image A illustrates a normal architecture of the dermal and epidermal layers as well as subcutaneous tissue of the skin. Sub-image B illustrates ear tissue from Croton oil-alone treated rats exhibiting severe inflammatory cell infiltration, extravasations and edema. Sub-images C–F; correspond to Compounds 1, 2, 3, and 4 respectively. Sub-image G corresponds to Indomethacin groups. Plates from C to F exhibit mild to moderate neutrophil infiltration, collagen fiber dispersion, and edema (40×).**

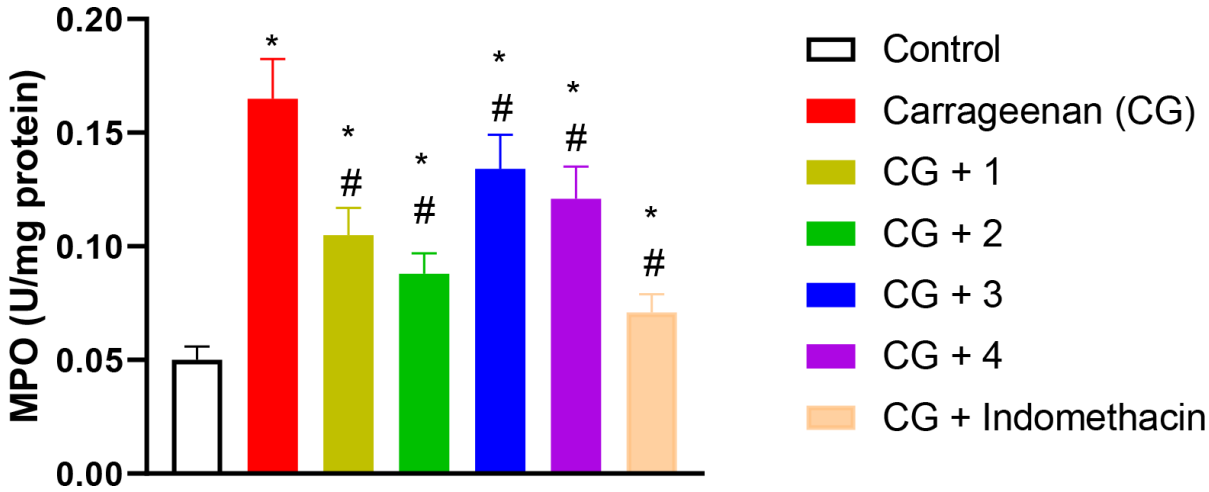

Fig. 5 **Effect of the isolated compounds on MPO activity in ear tissues of croton oil-induced rats. * Statistically significant from the control group at $P < 0.05$. # Statistically significant from the Carrageenan-induced group at $P < 0.05$.**

Table 5. **Effect of the isolated compounds on the weight of Croton oil-induced ear edema in rats**

Group	Ear punch weight (mg)	Ear punch weight (% of Control)
Control	21.30 ± 1.61	100
Croton oil (CO)	48.50* ± 3.70	227.7
CO + 1	45.3* ± 2.86	212.7
CO + 2	35.10 *, # ± 2.05	164.8
CO + 3	47.70* ± 3.11	223.5
CO + 4	41.6*, # ± 3.17	195.3
Indomethacin (10mg/Kg)	29.7*, # ± 1.80	139.4

compound **2** is an unsaturated derivative of compound **1**. The up-field shift of the carbonyl carbon signal to 198.5 ppm indicated the presence of conjugation, together with the appearance of a down-field methyl protons resonating at δ_H 1.90 indicated the location of the double bonds at C1–C10 and C7–C8. Comparison of the spectral data of compound **2** with the data reported by Jakupovic et al 1987, revealed that compound 2 can is identified as 9-Oxohumula-1(10)(*Z*),4,7(*E*)-trien-6,15-olide (**2**).

Compound **3** was isolated as colourless oil material. The molecular formula, $C_{15}H_{24}O$, was deduced from HRESIMS. ^{1}H-NMR spectrum indicated the presence of two olefinic protons resonating at δ_H 5.86 and 5.11 ppm, three quaternary methyl signals at 1.93, 1.68, and 1.60, and a secondary methyl at 0.79 (J = 6.9 Hz). ^{13}C-NMR spectrum showed

Table 6. **The binding affinity of compounds 1–4 to targeted proteins.**

Protein target	PDB ID	Binding affinity (kcal/mol)				
		Compounds				Control/standard drug (Indomethacin)
		1	2	3	4	
TNFα	2AZ5	–7.30	–7.31	–6.67	–6.95	–7.83
COX-2	4OTJ	–6.02	–7.49	–6.59	–6.11	–7.46
MPO	1CXP	–6.86	–7.59	–6.90	–6.98	–8.19
MAPK	1A9U	–6.67	–6.97	–6.92	–6.86	–7.74
5-LOX	3V99	–6.58	–6.65	–6.80	–6.67	–7.33
COX-1	4O1Z	–7.80	–7.70	–7.80	–7.61	–8.74

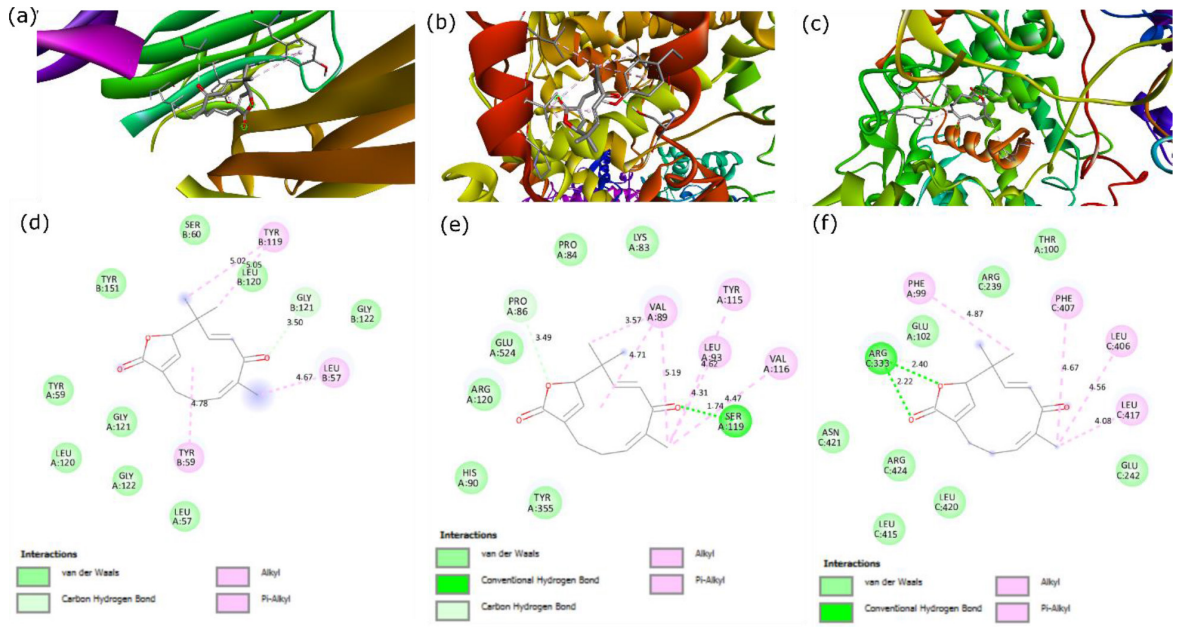

Fig. 6 **Docking visualization of compound 2 to TNFα (2AZ5), COX-2 (4OTJ), and MPO (1CXP) in 3D (a–c) and 2D (d–f), respectively.**

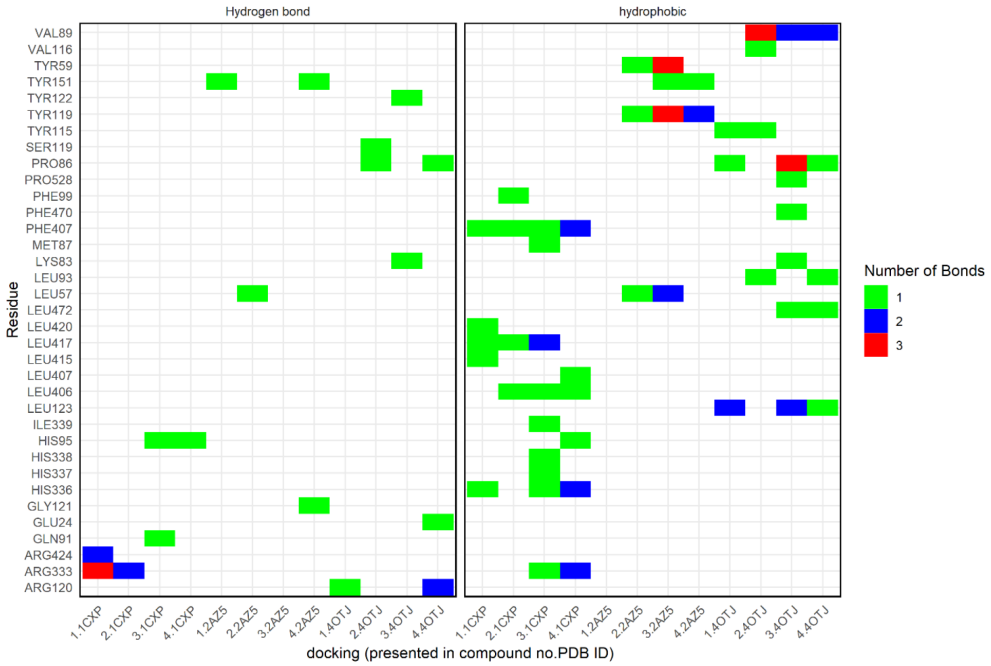

Fig. 7 **The number of bonds that appeared in the docking of compounds 1–4 TNFα (2AZ5), COX-2 (4OTJ), and MPO (1CXP), and the bond types as hydrogen bond (left) or hydrophobic interaction (right).**

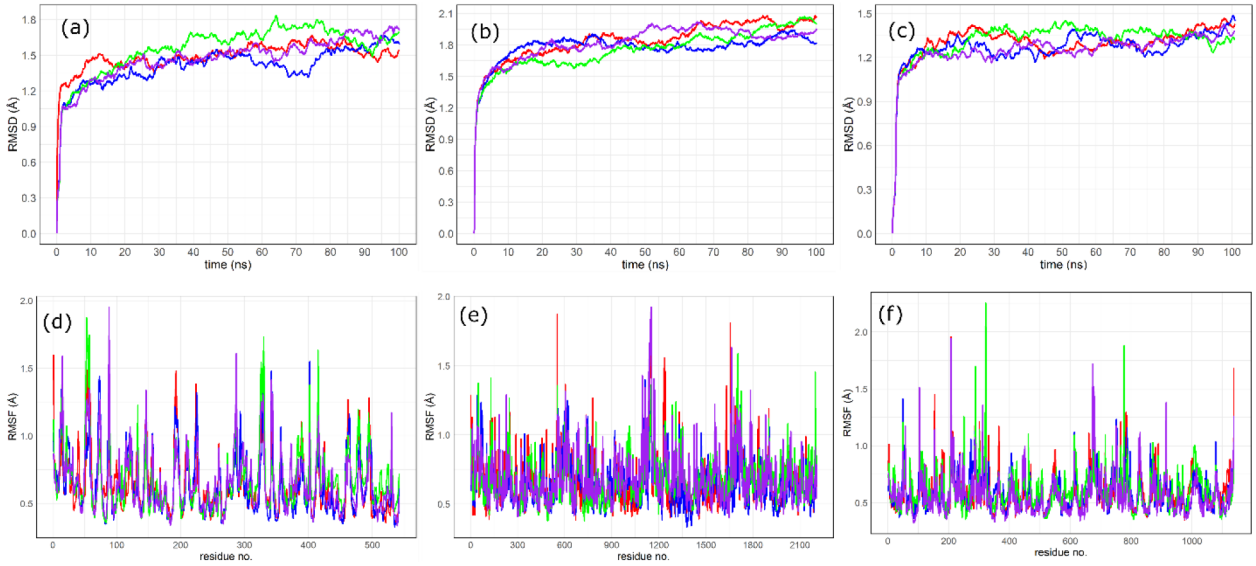

Fig. 8 **RMSD data (a–c) and RMSF data (d–f) of molecular dynamic simulation between compounds 1–4 to TNFα (2AZ5), COX-2 (4OTJ), and MPO (1CXP), respectively.**

Table 7. **The selected protein, PDB ID, and the RMSD of redocking of native ligand**

Protein target	PDB ID	Resolution (Å)	RMSD redocking native ligand (Å)
Tumor necrosis factor alpha (TNFα)	2AZ5	2.10	1.244
Cyclooxygenase-2 (COX-2)	4OTJ	2.11	1.371
Human myeloperoxidase (MPO)	1CXP	1.80	0.885
p38α MAP kinase (MAPK)	1A9U	2.50	0.025
S663D stable-5-lipoxygenase (5-LOX)	3V99	2.25	1.091
Cyclooxygenase-1 (COX-1)	4O1Z	2.40	1229

fifteen carbon signals including a signal due to α,β-unsaturated carbonyl absorbing at 201.2, and four signals at 161.3, 131.5, 127.2, and 124.3 attributed to two carbon-carbon double bonds. The presence of a monocyclic structure was deduced from the measured molecular formula and the ^{13}C-NMR spectral data. The obtained spectral data referred to the presence of a bisabolene-type sesquiterpene. Matching the obtained spectral data with those in literature referred to the isolation of the compound bisabola-2,10-dien-1-one (**3**) previously reported by.[17]

Compound **4** was isolated as colourless oil material. The molecular formula, $C_{15}H_{24}O_2$, was deduced from HRESIMS. Compound **4** is sixteen mass units more than compound **3**, which assigned the presence of an oxygenated function in **4**. ^{1}H-NMR spectrum indicated the presence of two olefinic protons resonating at δ_H 5.86 and 4.98 ppm, three quaternary methyl signals at 1.95, 1.68, and 1.60, and a secondary methyl at 1.02 (J = 6.5 Hz). ^{13}C-NMR spectrum showed fifteen carbon signals including a signal due to α,β-unsaturated carbonyl absorbing at 203.0, four signals at 162.6, 131.4, 124.3, and 123.2 attributed to two carbon-carbon double bonds, together with a signal due oxygenated quaternary carbon resonating at δ_C 77.0 ppm. The presence of a monocyclic structure was deduced from the measured molecular formula and the ^{13}C-NMR spectral data. The location of the hydroxyl group was evidenced from the change in both chemical shift and multiplicity of both C-1 and C-7 (Tables 1 and 2). The obtained spectral data referred to the presence of a bisabolene-type sesquiterpene. Matching the obtained spectral data with those in literature referred to the isolation of the compound 6-hydroxybisabola-2,10-dien-1-one (**4**) previously reported by Eldahmy et al., 1985.

Inflammation is a crucial response provided by the immune system to ensure the survival during infection, tissue injury and exposure to noxious conditions.[18] Although it is a physiological process, inflammation has been linked to the progression of many common diseases.[19] The aim of the present work was to evaluate the potential anti-inflammatory effects of 4 compounds isolated from Asteriscus graveolens. Carrageenin-induced paw edema model has been used as an initial study to characterize promising compounds. This model has long been used to assess the anti-inflammatory properties of new molecules.[20] Our data indicated that the isolated compounds could reduced paw edema. In particular, compound 2 showed the highest activity. These data were confirmed by histopathological examinations that clearly indicated inhibition of dermal necrosis and infiltration by mononuclear inflammatory cells. This was associated with potent inhibition of COX-2 and TNF-α release in the paw edema. COX-2 has been reported to have a pivotal role in inflammation.[21] these data gain support by the ability of sesquiterpens to inhibit COX-2 experimentally. Compounds 2 & 4 and indomethacin significantly inhibited its release into paw edema fluid. Interestingly, TNF-α is a central cytokine in inflammatory reactions.[22] In addition, biologics that neutralize TNF-α are among the most successful drugs for the treatment of inflammatory and autoimmune diseases.[23] Our data are consistent with previous studies highlighting the anti-inflammatory activity of sesquiterpenes.[24,25] It is noteworthy to report the observed anti-inflammatory activity of compound 2 that was comparable to those of indomethacin. This is consistent with molecular docking and

molecular dynamic simulation of compounds 1–4 to TNFα (PDB ID: 2AZ5), COX-2 (PDB ID: 4OTJ), and MPO (PDB ID: 1CXP). In the docking experiment, compound 2 showed the strongest affinity to these proteins of which the presence of carbonyl moiety established a strong hydrogen bond to the protein. Interestingly, based on the docking experiment, other pathways such as COX-1, 5-LOX, and MAPK pathways may be present in the anti-inflammatory activity of these compounds.

The observed anti-inflammatory activity of the isolated sesqueterpenes were confirmed in a croton oil-induced inflammation in rat ears. The model is well-known and is being used to screen preventive activities in acute inflammation.[26] In this study, ear punch weights were significantly reduced by the topical application of the isolated compounds. The same trend was observed through the 4 compounds. These data were assured by histopathological examinations that indicated severe inhibition of edema accumulation, extravasation and neutrophil infiltration. These histological studies are supported by the ability of the compound to inhibit MPO activity in ear tissues. This enzyme is a heme-containing peroxidase expressed mainly in neutrophils and monocytes and a hallmark of inflammatory response.[27] This gains support by previous reports highlighting the ability of sesqueterpenes and sesqueterpene lactones to exert anti-inflammation via inhibition of neutrophil infiltration as well as MPO release.[28,29]

Materials and Methods

Extraction and Isolation

General experimental procedures

TLC analyses were carried out on Silica gel 60 G F_{254} (0.20 mm) (20 × 20cm) (Macherey-Nagel). Column chromatography was packaged with silica gel 60 (70–230 mesh, Grade 60; 63 to 200 μm) (Merck), using analytical grade purity solvents (Honeywell and Sigma). A precoated TLC plates SIL G-25 UV254 layer, 0.25 mm thick silica gel 60 with fluorescent indicator UV254 (20 × 20cm) was using for preparative thin layer chromatography (PTLC) analysis. Compounds were detected by UV light (254 nm) and MeOH/H_2SO_4 reagent followed by heating. 1D and 2D on NMR was recorded in $CDCl_3$ on BRUKER Unity INOVA 850 instruments at the Department of Chemistry, Faculty of Science, King Abdulaziz University Jeddah, Saudi Arabia.

Chemicals

Indomethacin, carrageenan sodium, and croton oil were purchased from Merck (Darmstadt, Germany). The chemical solvents used for the extraction, elution and isolation process were *n*-hexane, benzene, ethyl acetate, ethanol (Honeywell and Sigma Aldrich).

Plant material

The whole plants of *Asteriscus graveolens* were collected in the flowering stage in the area of Arar, located in northern part of Saudi Arabia (30° 54′13.0″N41° 00′15.7″E) in March 2022. A voucher specimen was deposited in the collection of Chemistry Department, Faculty of science, King Abdulaziz University, Jeddah, Saudi Arabia.

Extraction and Isolation of Asteriscus graveolens

432.0 g of the air-dried plant, *A. graveolens*, were extracted in a mixture of methanol/methylene chloride solvents (1:2, v/v) and allowed to stand at room temperature for 72h. Filtration and concentration to exhaustion provided a viscous oily residue (10.3g). The obtained oily residue was defatted using the methanol freezing technique. The defatted residue was subjected to an open column chromatographic fractionation on a silica gel 60 G adsorbent using hexane/diethylether gradient elution. Fractions of ~ 25 ml each were collected. Fraction (**I**) 17–23 which were eluted by hexane-EtOAc (85:15) were combined. Purification by PTLC using 10% EtOAc in hexane, (R_f = 0.41) afforded a pure compound **3** (38mg). The fractions (**II**) 49–55 which were eluted by hexane/EtOAc (7.5:2.5) were combined. Purification by PTLC using 25% EtOAc in hexane (R_f = 0.48) afforded a pure compound **4** (46mg). The fractions (**III**) 107–119 which were eluted by hexane/EtOAc (7:3) were combined (400 mg). Purification of fraction III employing PTLC eluted with a mixture of benzene/EtOAc (9:1, v/v). The first band (R_f = 0.73) was purified by PTLC using 30% EtOA in hexane afforded two pure substances **1** (21mg) (R_f = 0.60) and **2** (20mg) (R_f = 0.56).

In vivo experiments

Animals

Male Sprague-Dawley rats were obtained from the animal facility of the South Valley University, and acclimatized for 7 days prior to experimentation. They were kept in a controlled temperature (21 ± 2°C), under a 12-h light/ dark cycle and fed *ad libitum* with free access to water. Animal handling was approved by the Ethics Committee, Faculty of Pharmacy, South Valley University, Quena, Egypt (P.S.V.U 223).

Carrageenin-induced rat paw edema

Forty-two male Sprague-Dawley (150 g ± 10 g) were randomly divided into 7 groups assigned Latin numbers I–VII. Rats were fasted, with free access to water, 15 h before the experiment. Groups I and II were given 1% DMSO in normal saline by intragastric tube, while groups III to VI received compounds **1**, **2**, **3 and 4** (orally, dissolved in 1% DMSO, 10 mg/Kg). Rats in group VII were treated orally with indomethacin as a reference anti-inflammatory compound (10 mg/kg). Half an hour after oral treatment, group I received .05 ml saline, while groups II–IX received 0.05 mL carrageenin (1% solution in saline sc) on the plantar surface of the right hind paw. The right hind paw volume was determined at 3 h after carrageenin injection by solution displacement using UGO-BASILE 7140 plethysmometer (Comerio, Italy). This was followed by animal sacrifice by decapitation.[26] The selected doses and time of measurement were based on a pilot study in our laboratory. Edema samples were withdrawn for assessment of tumor necrosis factor-alpha (TNF-α) concentration. Then paws were kept in 10% neutral formalin for histopathological examinations.

Croton oil-induced ear edema

The study was carried out according to the procedure described by Wen-Guang et al. (2001).[30] An irritant solution was prepared by dissolving 4 parts croton oil (the irritant) in

a solvent mixture of 10 parts ethanol, 20 parts pyridine, and 66 parts diethyl ether. The isolated compounds (**1, 2, 3,** and **4**) and indomethacin, were dissolved in the same vehicle of the irritant. A concentration of 1 mg/100 mL was prepared for each isolated compound. Indomethacin was used in a concentration of 12.5% (w/v).[30]

Additional forty-two male Sprague-Dawley (150 g ± 10 g) were divided into 7 groups as previously described above. The irritant, four isolated compounds, and indomethacin solutions were applied in volume of 20 µL topically on both sides of the right ears. The left of each rat was kept untreated to serve as a control. Group I received only the irritant-free solvent mixture and served as negative control. Groups III to VI received the isolated compounds and group VII received indomethacin solution. After sixty munites, groups II–VII received croton oil solution and group I was re-administered the croton oil-free solvent mixture again. After 4h, the animals were sacrificed by decapitation. An 8-mm cork borer was used to punch out discs from both the treated as well as the control ears. The two punches were weighed immediately and the difference in weight was used to assess the inflammatory response. Representative ear punches were kept in 10% neutral formalin for histopathological examinations. The rest of ear punches were flash frozen in liquid nitrogen and then kept at -80°C for assessment of myeloperoxidase (MPO).

Histopathological examination

Rat paw and ear specimens were fixed in 10% neutral buffer formalin for 4h h. Then tissues were trimmed, dehydrated in ascending concentrations of ethyl alcohol and cleared in xylene. This was followed by embedding in paraffin. Thin sections (5 µm) were processed and stained with Hematoxylin & Eosin stain.[31]

Assessment of COX-2, TNF-α and MPO

Cyclooxygenase-2 (COX-2) and tumor necrosis factor-α (TNF-α) concentration in collected rat paw edema was assayed using a commercial kit obtained from MyBioScource (Catalog # MBS266603 and MBS2507393 respectively, San Diego, CA, USA). MPO content of ear tissues was determined as previously described by.[26] Protein content was assessed using BCA Protein Assay Kit (Catalog #K813; BioVision, Milpitas, CA, USA).

In silico study

Molecular docking

Molecular docking of compounds **1–4** was performed on the target proteins used in the in vitro study. The PDB IDs of TNFα, COX-2, and MPO are provided in Table 7. Additionally, docking was conducted with MAPK, 5-LOX, and COX-1 to explore alternative pathways. The docking of compounds **1–4** to these proteins was carried out using MGL Tools 1.5.7, AutoGrid4, and AutoDock4. The compounds were sketched using the MarvinJS webserver (https://marvinjs-demo.chemaxon.com/), while the protein structures were downloaded from the RCSB PDB webserver (https://www.rcsb.org/). Prior to docking, the proteins were prepared using MGL Tools, with water molecules removed, hydrogens added, and Gasteiger charges computed. Grid maps were generated using MGL Tools, and docking parameters were set using the Lamarckian Genetic Algorithm. The docking was then performed using AutoGrid4 and AutoDock4.[32] To validate the docking process, redocking of native ligands was conducted for each protein, and the resulting RMSD values (RMSD < 2 Å) confirmed the accuracy of the docking procedure. Visualisation of the docking results was carried out for the compound-protein interactions exhibiting the strongest binding affinities, focusing on proteins involved in the in vitro study. Additionally, the presence and type of bonds between other compound-protein interactions, along with the number of bonds, were presented in a heatmap generated using RStudio.

Molecular dynamic simulation

Molecular dynamics (MD) simulations for compounds 1–4 in complex with TNFα (PDB ID: 2AZ5), COX-2 (PDB ID: 4OTJ), and MPO (PDB ID: 1CXP) were performed using NAMD, with VMD utilized for analysis. Prior to the simulations, the proteins and compounds were prepared via the CHARMM-GUI platform (https://charmm-gui.org).[33,34] Energy minimisation and system equilibration were completed before beginning the 100-nanosecond MD simulations, which were conducted with periodic boundary conditions (PBCs) in place. The simulations employed a 2-femtosecond time step, with temperature managed by a Langevin thermostat and pressure controlled through the Nose–Hoover Langevin piston method.[35,36]

Statistical analysis

Data analysis was performed using one-way ANOVA followed by the post-hoc test, Tukey using GraphPad Prism ver 8.0. (San Deigo, CA, USA). Results are presented as means and standard deviation (SD). *P* values less than 0.05 indicate that differences among the treatment groups are statistically significant.

Conclusions

The humulene-type sesquiterpenoids from *Asteriscus graveolens* showed an anti-inflammatory activity based on *in vivo* using Sprague-Dawley rat and *in silico* study. The activity was attributed to the compounds' inhibition via TNFα, COX-2, and MPO pathways. The in vivo exhibited histopathological examinations that indicated inhibition of dermal necrosis and infiltration by mononuclear inflammatory cells. While the in *in silico* analysis demonstrated the docking stability of docking within 100 ns. In addition, other pathways may contribute to the anti-inflammatory activities of compounds **1–4**.

Author Contributions

Conceptualization, W.M.A. and A.B.A.; methodology, H.S.A. and W.M.A.; validation, H.S.A., A.B.A. and W.M.A.; formal analysis, F.A.A., H.A., F.B.A., and F.B.; investigation, F.A.A, H.A., E.M.A. and F.B.; resources, H.S.A. and H.A..; data curation, F.A.A, F.B.A, and F.B.; writing—original draft preparation, F.A.A., F.B.A., and F.B.; writing—review and editing, E.M.A., H.S.A, A.B.A., W.M.A.; visualization, A.B.A. and F.B.; supervision, A.B.A. and W.M.A. All authors contribute equally as the main author to this publication. All authors have read and agreed to the published version of the manuscript.

Funding

This research received no external funding.

Institutional Review Board Statement

Animal handling was approved by Ethics Committee, Faculty of Pharmacy, South Valley University, Quena, Egypt (P.S.V.U 223).

Informed Consent Statement

Not applicable.

Data Availability Statement:

The data that supports the findings of this study are available from the corresponding author upon request.

Acknowledgments

The authors acknowledge the Department of Chemistry and Faculty of Pharmacy, South Valley University, for the facility.

Conflicts of Interest

The authors declare no conflicts of interest.

References

1. Debnath, T.; Kim, D.H.; Lim, B.O. Natural products as a source of anti-inflammatory agents associated with inflammatory bowel disease. *Molecules* 2013, 18, 7253–7270. https://doi.org/10.3390/molecules18067253.
2. Gautam, R.; Jachak, S.M. Recent developments in anti-inflammatory natural products. *Med. Res. Rev.* 2009**,** 29, 767–820. https://doi.org/10.1002/med.20156.
3. Da Silveira e Sá, R.D.C.; Andrade, L.N.; De Sousa, D.P. A review on anti-inflammatory activity of monoterpenes. *Molecules* 2013**,** 18, 1227–1254. https://doi.org/10.3390/molecules18011227.
4. Azab, A.; Nassar, A.; Azab, A.N. Anti-inflammatory activity of natural products. *Molecules* 2016, 21, 1321. https://doi.org/10.3390/molecules21101321.
5. Cristofari, G.; Znini, M.; Majidi, L.; Mazouz, H.; Tomi, P.; Costa, J.; Paolini, J. Chemical diversity of essential oils from *Asteriscus graveolens* (Forssk.) Less.: Identification of cis-8-acetoxychrysanthenyl acetate as a new natural component. *Chem. Biodivers.* 2012, 9, 727–738. https://doi.org/10.1002/cbdv.201100118.
6. Benomari, F.Z.; Dib, M.E.A.; Muselli, A.; Costa, J.; Djabou. N. Comparative study of chemical composition of essential oils for two species of Asteriscus genus from Western Algeria. *J. Essent. Oil. Res.* 2019, 31, 414–424. https://doi.org/10.1080/10412905.2019.1579761.
7. Chaib, F.; Allali, H.; Bennaceur, M.; Flamini, G. Chemical composition and antimicrobial activity of essential oils from the aerial parts of *Asteriscus graveolens* (Forssk.) Less. and *Pulicaria incisa* (Lam.) DC.: Two asteraceae herbs growing wild in the Hoggar. *Chem. Biodivers.* 2017, 14, e1700092. https://doi.org/10.1002/cbdv.201700092.
8. Helmy, S.N.; Ezzat, S.R.; Naguib, M.H. Antioxidant, antibacterial activities and phytochemical screening of *Asteriscus pygmaeus* aerial parts ethanolic extract. *GSC Biol. Pharm. Sci.* 2019, 9, 041–046. https://doi.org/10.30574/gscbps.2019.9.3.0218.
9. Triana, J.; Eiroa, J.L.; Morales, M.; Perez, F.J.; Brouard, I.; Quintana, J.; Ruiz-Estévez, M.; Estévez, F.; León, F. Sesquiterpenoids isolated from two species of the *Asteriscus Alliance*. *J. Nat. Prod.* 2016, 79, 1292–1297. https://doi.org/10.1021/acs.jnatprod.5b01013.
10. Farah, R.; Mahfoud, H.M.; Mohamed, D.O.H.; Amoura; Roukia, H.; Naima, H.; Houria, M.; Imane, B.; Chaima, B. Ethnobotanical study of some medicinal plants from Hoggar, Algeria. *J. Med. Plants. Res*. 2015, 9, 820–827. https://doi.org/10.5897/jmpr2015.5805
11. Belhadi, F.; Ouafi, S.; Bouguedoura, N. Phytochemical composition and pharmacological assessment of callus and parent plant of *Asteriscus graveolens* (Forssk.) Less. from Algerian Sahara. *Trop. J. Pharm. Res.* 2020, 19, 1895–1901. https://doi.org/10.4314/tjpr.v19i9.14.
12. Znini, M.; Cristofari, G.; Majidi, L.; Mazouz, H.; Tomi, P.; Paolini, J.; Costa, J. Antifungal activity of essential oil from *Asteriscus graveolens* against postharvest phytopathogenic fungi in apples. *Nat. Prod. Commun.* 2011, 6, 1763–1768. https://doi.org/10.1177/1934578x1100601147.
13. Hammoud, L.; León, F.; Brouard, I.; Gonzalez-Platas, J.; Benayache, S.; Mosset, P.; Benayache, F. Humulene derivatives from Saharian *Asteriscus graveolens*. *Tetrahedron Lett.* 2018, 59, 2668–2670. https://doi.org/10.1016/j.tetlet.2018.05.079.
14. Rauter, A.P.; Branco, I.; Bermejo, J.; Gonzáles, A.G.; García-Grávalos, M.D.; Feliciano, A.S. Bioactive humulene derivatives from *Asteriscus vogelii*. *Phytochemistry* 2001, 56, 167–171.
15. Imieje, V.O.; Zaki, A.A.; Metwaly, A.M.; Eissa, I.H.; Elkaeed, E.B.; Ali, Z.; Khan, I.A.; Falodun, A. Antileishmanial derivatives of humulene from *Asteriscus hierochunticu*s with in silico tubulin inhibition potential. *Rec. Nat. Prod.* 2022, 16, 150–171. https://doi.org/10.25135/rnp.253.21.01.1945.
16. Jakupovic, J.; Lehmann, L.; Bohlmann, F.; Hogdson, A. Nerolidol derivatives from *Asteriscus sericeus*. *Phytochemistry* 1987, 26, 2854–2855.
17. Dahmy, S. El.; Jakupovic, J.; Bohlmann, F.; Sarg, T. New humulene derivatives from *Asteriscus graveolens. Tetrahedron* 1985, 41, 309–316.
18. Ahmed, A.U. An overview of inflammation: Mechanism and consequences. *Front. Biol. China* 2011, 6, 274–281. https://doi.org/10.1007/s11515-011-1123-9.
19. Krishnamoorthy, S.; Honn, K.V. Inflammation and disease progression. *Cancer Metastasis Rev.* 2006, 25, 481–491. https://doi.org/10.1007/s10555-006-9016-0.
20. Whiteley, P.E.; Dalrymple, S.A. Models of inflammation: Carrageenan-induced paw edema in the rat. *Curr. Protoc. Pharmacol.* 2001, 00:5.4.1-5.4.3
21. Cui, J.; Jia, J. Natural COX-2 inhibitors as promising anti-inflammatory agents: An update. *Curr. Med .Chem.* 2021, 28, 3622–3646. https://doi.org/10.2174/1875533xmtewdmdin5.
22. van Loo, G.; Bertrand, M.J.M. Death by TNF: A road to inflammation. *Nat. Rev. Immunol.* 2023, 23, 289–303. https://doi.org/10.1038/s41577-022-00792-3.
23. Agmon-Levin, N.; Mosca, M.; Petri, M.; Shoenfeld, Y. Systemic lupus erythematosus one disease or many? *Autoimmun Rev.* 2012, 11, 593–595. https://doi.org/10.1016/j.autrev.2011.10.020.
24. Lajter, I.; Vasas, A.; Béni, Z.; Forgo, P.; Binder, M.; Bochkov, V.; Zupkó, I.; Krupitza, G.; Frisch R.; Kopp, B.; Hohmann, J. Sesquiterpenes from *Neurolaena lobata* and their antiproliferative and anti-inflammatory activities. *J. Nat. Prod.* 2014, 77, 576–582. https://doi.org/10.1021/np400834c.
25. Hai, C.T.; Luyen, N.T.; Giang, D.H.; Minh, B.Q.; Trung, N.Q.; Chinh, P.T.; Hau, D.V.; Dat, N.T. *Atractylodes macrocephala* rhizomes contain anti-inflammatory sesquiterpenes. *Chem. Pharm. Bull*. 2023, 71, 451–453. https://doi.org/10.1248/cpb.c22-00779.
26. Gábor, M. Carrageenan-induced paw edema in the rat and mouse. In *Winyard PG, Willoughby DA (eds) Methods in molecular biology: Inflammation protocols methods in molecular biology*. Humana Press Inc., Totowa: New Jersey, 2003, pp 129–138
27. Aratani, Y. Myeloperoxidase: Its role for host defense, inflammation, and neutrophil function. *Arch. Biochem. Biophys*. 2018, 640, 47–52. https://doi.org/10.1016/j.abb.2018.01.004.
28. Hayley, C.; Stephen, R.Z.; Sarah, F.; Billie, G-C.; Fiona, B.; Lisa, W.; Matthew, K.; Sally, B.; Stephen, H.; Bryan, B. The influence of the neighborhood physical environment on early child health and development: A review and call for research. *Heal Place* 2015, 33, 25–36.
29. Paço, A.; Brás, T.; Santos, J.O.; Sampaio, P.; Gomes, A.C.; Duarte, M.F. Anti-inflammatory and immunoregulatory action of sesquiterpene lactones. *Molecules* 2022, 27, 1142. https://doi.org/10.3390/molecules27031142.
30. Wen-Guang, L.; Xiao-Yu, Z.; Yong-Jie, W.; Xuan, T. Anti-inflammatory effect and mechanism of proanthocyanidins from grape seeds. *Acta Pharmacol. Sin.* 2001, 22, 1117–1120.
31. Bancroft, J.D.; Marilyn, G. Theory and Practice of Histological Techniques, 6th ed. Churchill Livingstone: London, 2008.
32. Trott, O.; Olson, A.J. AutoDock Vina: Improving the speed and accuracy of docking with a new scoring function, efficient optimization, and

multithreading. *J. Comput. Chem.* 2009, 31, 455–461. https://doi.org/10.1002/jcc.21334.
33. Lee, J.; Cheng, X.; Swails, J.M.; Yeom, M.S.; Eastman, P.K.; Lemkul, J.A.; Wei, S.; Buckner, J.; Jeong, J.C.; Qi, Y.; Jo, S.; Pande, V.S.; Case, D.A.; Brooks, C.L.; MacKerell, A.D.; Klauda, J.B.; Im, W. CHARMM-GUI input generator for NAMD, GROMACS, AMBER, OpenMM, and CHARMM/OpenMM simulations using the CHARMM36 additive force field. *J. Chem. Theory Comput*. 2016, 12, 405–413. https://doi.org/10.1021/acs.jctc.5b00935.
34. Jo, S.; Kim, T.; Iyer, V.G.; Im, W. CHARMM-GUI: A web-based graphical user interface for CHARMM. *J. Comput. Chem.* 2008, 29, 1859–1865. https://doi.org/10.1002/jcc.
35. Phillips, J.C.; Braun, R.; Wang, W.; Gumbart, J.; Tajkhorshid, E.; Villa, E.; Chipot, C.; Skeel, R.D.; Kalé, L.; Schulten, K. Scalable molecular dynamics with NAMD. *J. Comput. Chem.* 2005, 26, 1781–1802. https://doi.org/10.1002/jcc.20289.
36. Humphrey, W.; Dalke, A.; Schulten, K. VMD: Visual molecular dynamics. *J. Mol. Graph*. 1996, 14, 33–38.